

ENVIRONMENTAL SCIENCE

Canopy near-infrared reflectance and terrestrial photosynthesis

Grayson Badgley,^{1,2*} Christopher B. Field,^{1,2} Joseph A. Berry¹

Global estimates of terrestrial gross primary production (GPP) remain highly uncertain, despite decades of satellite measurements and intensive in situ monitoring. We report a new approach for quantifying the near-infrared reflectance of terrestrial vegetation (NIR_V). NIR_V provides a foundation for a new approach to estimate GPP that consistently untangles the confounding effects of background brightness, leaf area, and the distribution of photosynthetic capacity with depth in canopies using existing moderate spatial and spectral resolution satellite sensors. NIR_V is strongly correlated with solar-induced chlorophyll fluorescence, a direct index of photons intercepted by chlorophyll, and with site-level and globally gridded estimates of GPP. NIR_V makes it possible to use existing and future reflectance data as a starting point for accurately estimating GPP.

INTRODUCTION

Photosynthesis by terrestrial vegetation is the primary driver of multiple global biogeochemical cycles. As a result, quantifying photosynthesis [or gross primary production (GPP)] at the global scale has implications for our understanding of global change, biodiversity, and agriculture. Satellite remote sensing, through regular global measurements, has markedly improved estimates of the productivity of the biosphere (1, 2). While the biochemistry of photosynthesis at the leaf scale is well characterized (3), ecosystem and regional estimates remain highly uncertain (4).

Here, we describe an approach to address two of the more vexing challenges in estimating GPP from remote sensing. The first challenge is the mixed-pixel problem; vegetation remote sensing requires determining the fraction of the surface that is vegetated and reconstructing the signal attributable to vegetation (5). The spatial resolution of current sensors (ranging from several meters to tens of kilometers) means that pixels are almost always a mixture of vegetated and nonvegetated surfaces (for example, bare soil, branches, and litter). One possible strategy for dealing with mixed pixels is increased spatial resolution, providing a strong motivation for enhancing the spatial resolution of future satellites. The second challenge is determining the photosynthetic capacity of vegetation. The number, organization, and chemistry of leaves within the canopy all influence canopy photosynthetic capacity (6, 7).

The approach we present here addresses both of these challenges and, as a consequence, provides a robust approach for estimating GPP from remote sensing. The new index, the near-infrared reflectance of vegetation (NIR_V), is the product of total scene NIR reflectance (NIR_T) and the normalized difference vegetation index (NDVI), a common measure of vegetation cover. From a physical perspective, NIR_V represents the proportion of pixel reflectance attributable to the vegetation in the pixel. We present evidence of a general NIR_V -GPP relationship in four steps (see Materials and Methods for additional details on choice of analytical methods). First, an analysis of canopy radiation transport provides a theoretical foundation relating the product of NDVI and NIR_T to NIR_V . Because NIR_V isolates the vegetated signal, it eliminates much of the mixed-pixel problem. Second, a comparison of NIR_V with solar-induced chlorophyll fluorescence (SIF), a relatively new satellite mea-

surement that is insensitive to background contamination, documents the global-scale relationship between NIR_V and canopy development. Third, correlations between NIR_V and monthly measured and globally modeled GPP establish the generality and the strength of the NIR_V -GPP relationship. Fourth, published data from many studies help explain why NIR_V addresses not only the mixed-pixel problem but also aspects of photosynthetic capacity.

RESULTS AND DISCUSSION

Sellers and coworkers used a two-stream approximation model to demonstrate that NDVI is a useful proxy for the fraction of photosynthetically active radiation (fPAR) absorbed by a canopy (8–10). Sellers pointed out that the NIR reflectance attributable to vegetation should be a more robust proxy of fPAR than NDVI, if it were only possible to disentangle the vegetated signal from variations in nonvegetated background reflectance. Our results demonstrate that the product of NIR_T and NDVI better normalizes for variations in background reflectance than NDVI or NIR_T alone. With Sellers' two-stream approximation model, NIR_V has a stronger linear relationship with modeled fPAR across all possible soil reflectances ($R^2 = 0.99$) than the relationship of NDVI and fPAR ($R^2 = 0.95$; see text S1 and fig. S1). The difference in the two approaches is especially pronounced for low leaf areas. Results from a simplified two-dimensional (2D) reflectance model demonstrate that the product of NDVI and NIR_T captures the fraction of NIR reflectance attributable to vegetation (see text S2 and fig. S2).

An empirical test of this theoretical result comes from comparing NIR_V with SIF using GOME-2, a sensor capable of measuring both SIF and NIR_V simultaneously. SIF measures light emitted by chlorophyll, bypassing the challenge of discriminating between photons scattered by vegetated and nonvegetated surfaces (11). If our proposed index of NIR_V captures the fraction of NIR reflectance attributable to vegetation, then NIR_V should be highly correlated with SIF across all pixels, independent of vegetated fraction. On the basis of a global data set, monthly values of SIF strongly correlate with monthly NIR_T measurements over highly vegetated pixels. However, the correlation decreases with lower vegetated fraction (Fig. 1A). In contrast, SIF and NIR_V are highly correlated across all land sites at the monthly time scale (Fig. 1B). This agreement corroborates our theoretical results, demonstrating that NIR_V addresses the mixed-pixel problem, effectively isolating the proportion of reflectance attributable to vegetation. The link between SIF and NIR_V is also found in

2017 © The Authors, some rights reserved; exclusive licensee American Association for the Advancement of Science. Distributed under a Creative Commons Attribution NonCommercial License 4.0 (CC BY-NC).

¹Department of Global Ecology, Carnegie Institution for Science, Stanford, CA 94305, USA. ²Department of Earth System Science, Stanford University, Stanford, CA 94305, USA.

*Corresponding author. Email: badgley@stanford.edu

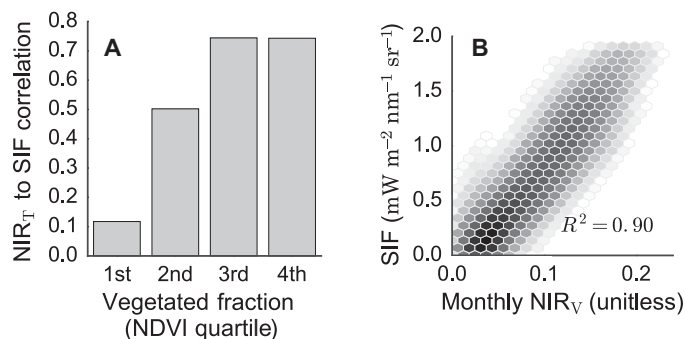


Fig. 1. SIF relates to NIR_V through surface vegetated fraction. (A) The correlation between NIR_T and SIF increases with vegetated fraction. The upper bounds of the NDVI quartiles are as follows: 0.17, 0.27, 0.37, and 0.72. (B) NIR_V closely proxies multiyear monthly averaged SIF. All data calculated using 2008–2010 GOME-2 data averaged monthly and regridded to 0.5°. Shading indicates the logged number of pixels within each bin.

radiation transport simulations (see text S3 and fig. S3). This further indicates that NIR_V should strongly relate to GPP, although NIR_V is likely determined solely by canopy structure. This contrasts with SIF, which should also contain physiological information through variations in fluorescence yield.

Much of the excitement about SIF relates to its strong correlation with GPP (12–15). Monthly average SIF at 0.5° spatial resolution strongly corresponds with state-of-the-art statistical estimates of monthly GPP ($R^2 = 0.73$, Fig. 2A) (16). However, available SIF measurements have limited spatial resolution (for example, 40 × 60 km²) and span a short duration, with measurements extending only back to 2007, limiting their potential applications. In contrast, numerous sensors have measured NIR_T and NDVI for the entire globe at moderate spatial resolution and regular intervals over several decades. Monthly NIR_V, calculated from nadir-corrected Moderate Resolution Imaging Spectroradiometer (MODIS) reflectances (17), has a higher correlation with globally gridded GPP than GOME-2 SIF ($R^2 = 0.91$; Fig. 2B). This strong agreement persists across all biomes, including sparsely vegetated ecosystems (for example, grasslands), where reflectance-based approaches traditionally yield high uncertainty (18), further emphasizing that NIR_V addresses the mixed-pixel problem. The ability of NIR_V to resolve the mixed-pixel problem arises from the combination of NDVI and NIR_T, as evidenced by the comparison of MODIS-derived NIR_T and NIR_V against measurements of SIF (fig. S4).

To more directly test the usefulness of NIR_V for estimating GPP, we compared MODIS-based NIR_V estimates with monthly observations of GPP at 105 in situ CO₂ flux monitoring sites (Fig. 3A) (19). Across all sites, the median value of monthly variance in observed GPP explained by NIR_V is 76% (Fig. 3B). For these sites, NIR_V explains more of the variance in monthly GPP estimates than either MODIS NDVI or fPAR. NIR_V performs as well as MODIS GPP estimates, although the MODIS GPP algorithm explicitly incorporates additional observations, including incident photosynthetically active radiation, temperature, and humidity, in addition to biome-specific terms, to account for the temperature sensitivity and water stress sensitivity of photosynthesis (20). This indicates that NIR_V relates to key parameters that determine GPP. Furthermore, the tightly clustered range of values for the slope of multiyear average monthly GPP as a function of multiyear average monthly NIR_V indicates that NIR_V captures parameters that control GPP over longer time scales as well (Fig. 3C).

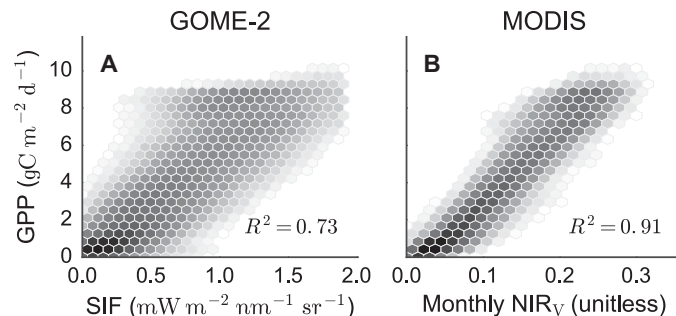


Fig. 2. Comparison of multiyear monthly mean (A) SIF and (B) NIR_V against global data-driven GPP estimates. SIF estimates come from GOME-2 data averaged monthly and regridded to 0.5°. MODIS NIR_V estimates were aggregated to 0.5° from 500-m scenes of BRDF-corrected reflectances. GPP estimates come from the Max Planck Institute upscaling approach (16). Shading indicates the logged number of pixels within each bin.

Canopies with high carbon assimilation rates (for example, crops) display leaves with high photosynthetic capacity to maximize direct beam radiation, resulting in higher NIR_V. A conifer canopy can have the same fPAR as a crop canopy but has a complex architecture with clumped and shaded leaves. This canopy has both a lower photosynthetic capacity and lower NIR_V. This pattern is evident across the 105 CO₂ monitoring sites examined in Fig. 3, with crop sites having both 60% higher NIR_V and GPP than evergreen sites during the month of peak GPP, despite the sites sharing similar fPAR values (see table S5). In this formulation, NIR_V describes the relationship between canopy light capture and GPP. Across the 105 sites we examined, canopies with higher NIR_V have higher light-use efficiencies.

A substantial body of literature supports the hypothesis that leaves are built and displayed in a way that matches energy absorption to photosynthetic capacity (6, 7, 21, 22). Because plants allocate photosynthetic capacity to optimize resources in a way that tends to fully exploit captured sunlight, the photochemical capacity of the complete canopy (including shaded leaves deep in the canopy) directly relates to the performance of the top leaves of the canopy (10). Canopies with high photochemical capacity can more readily avoid light saturation, meaning they should display their leaves to use a higher proportion of direct beam radiation. This configuration, driven by whole-canopy capacity, results in higher values of NIR_V. We hypothesize that NIR_V captures these variations in canopy architecture, which, in turn, are the end product of whole-plant optimizations, from the scale of the chloroplast upward. This theoretical interpretation of NIR_V as a proxy for photosynthetic capacity is further corroborated by a pair of studies that related NIR_T from high-resolution (17 m) Airborne Visible/Infrared Imaging Spectrometer (AVIRIS) imagery with leaf nitrogen content, the main determinant of photosynthetic capacity (23), and the ratio of sun-exposed leaf area to total leaf area across broadleaf and conifer forest plots in the northeastern United States (24). Like nitrogen content, the ratio of sun to shaded leaves is strongly related to photosynthetic capacity (25–27). The full extent and origin of the NIR_V-photosynthesis relationship should prove a fruitful area of future study (28).

The strong theoretical foundation of NIR_V, combined with its ease of calculation and applicability to decades of moderate-resolution, reflectance-based remote sensing data, will facilitate the study of GPP in natural and agricultural systems. NIR_V can also help quantify ecosystem responses to global change and spatial and temporal

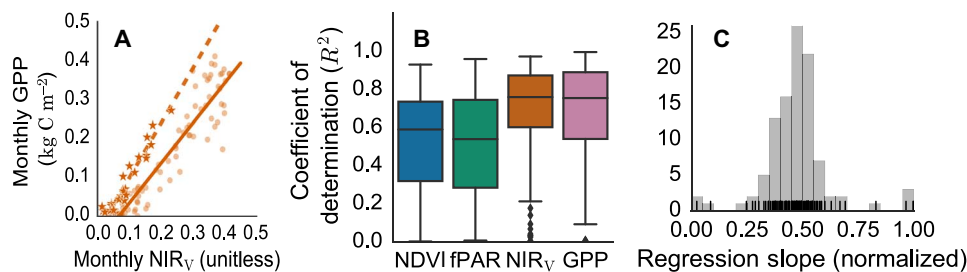


Fig. 3. Convergence of scaling between NIR_v and GPP. (A) For each site (two represented here), we fit a linear regression against average monthly GPP and the monthly value of MODIS NDVI, fPAR, GPP, and NIR_v (shown). (B) NIR_v explains more of the variation in monthly observed GPP than MODIS NDVI and fPAR. There is no significant difference in the performance of NIR_v and MODIS GPP across 105 FLUXNET sites. Whiskers denote the 5th and 95th percentile of site-level R^2 , with markers indicating outlying sites. (C) Slope parameter of site-level regressions (normalized between 0 and 1) of annual-average monthly NIR_v and annual-average monthly GPP from FLUXNET sites. Black lines represent the slope parameters of individual sites.

environmental variations. NIR_v explains a large fraction of the variance of GPP on monthly to annual time scales, paving the way toward improving our understanding of photosynthesis at the global scale.

MATERIALS AND METHODS

Data sets and processing

GOME-2 SIF.

We generated GOME-2 0.5° fluorescence at 740 nm and reflectance at 670 and 780 nm from level 2 data taken from the Aura Validation Data Center (AVDC) data archive (avdc.gsfc.nasa.gov) and described by Joiner *et al.* (29). For each month, we gridded all retrievals to a global 0.5° grid, excluding retrievals where the solar zenith angle exceeded 70° . All values of SIF were included in monthly estimates. After calculating multiyear monthly means, we discarded negative values of NDVI or SIF. We also excluded SIF retrievals exceeding the 99th percentile of the multiyear monthly mean from our analysis.

MODIS BRDF-corrected reflectances.

MODIS reflectance data were derived from the MCD43A4.005 BRDF-Adjusted Reflectance 16-Day L3 Global 500m product hosted on Google Earth Engine. To calculate monthly reflectance values, we first took the median of all available 16-day composite imagery at a 500-m scale. We then averaged together all 500-m median composite scenes falling within 0.5° pixels for the global analysis. We repeated this procedure for the FLUXNET sites, taking the average of all median composite scenes intersecting a 1-km-diameter circle centered on the latitude and longitude of each site. We used NDVI values already calculated by Google Earth Engine under the data collection entitled MCD43A4_NDVI.

MODIS vegetation indices and GPP estimates.

We calculated mean monthly NDVI, fPAR, and GPP for all FLUXNET sites, following the same procedure used for reflectance data (see above). All values were calculated using data collections hosted on Google Earth Engine. For GPP, we used 8-day L4 GPP estimates at 500-m resolution (MOD17A2H.006). For fPAR, we used 4-day L4 fPAR estimates at 500-m resolution (MCD15A3H.006).

FLUXNET data.

We used monthly GPP measurements from the July 2016 release of the Tier 1 FLUXNET2015 data product. More specifically, we used GPP calculated with variable USTAR filtering and daytime partitioning of fluxes (GPP_DT_VUT_MEAN).

Max Planck Institute GPP estimates.

We calculated the multiyear monthly mean of GPP at the 0.5° scale from data described by Beer *et al.* (16). We used the May 2012 release, downloaded from www.bgc-jena.mpg.de/geodb/projects/Data.php.

Analysis

General rationale.

Our analyses are based on reflectance values, which is in line with the data readily available from the satellite record. However, radiance values (the product of reflectance and the incident light) are probably the true basis for the correlations we describe. Because the light is approximately constant in the satellite measurements, reflectance measurements suffice. However, radiances should be used in studies (e.g., field measurements over the diurnal cycle) where light is variable.

GOME-2 and MODIS NIR_v calculation.

We calculated NIR_v as the product of monthly median NDVI and monthly median NIR reflectance. Before multiplication, we subtracted 0.08 from all NDVI values in an attempt to partially account for the NDVI of bare soil.

NIR_v , GOME-2 SIF, and MPI comparison.

We calculated the multiyear monthly mean of MODIS NIR_v , GOME-2 SIF, and MPI GPP from monthly estimates of each product, spanning from 2008 to 2010, which is the period where we calculated global NIR_v . We excluded all NIR_v values less than or equal to zero from the final comparison under the assumption that NIR_v should never take the value of zero. Although low values of NIR_v show a strong linear relationship with MPI GPP estimates, zero estimates exhibited almost no relationship to MPI, suggesting a problem in excluding invalid MODIS data.

FLUXNET comparison.

FLUXNET2015 data were compared with MODIS-derived NIR_v collected during the same month as the reported GPP measurement. No multiyear monthly means were used in this portion of the analysis, with the exception of Fig. 3C.

Open-source software.

All analyses, with the exception of the SCOPE simulations, were performed using the Python programming language. We processed netCDF files and tabular data using xarray (30) and pandas (31). We used NumPy (32) and SymPy (33) for numerical simulations, matplotlib (34) and seaborn (35) for visualization, and Jupyter notebooks for organizing analyses (36).

SUPPLEMENTARY MATERIALS

Supplementary material for this article is available at <http://advances.sciencemag.org/cgi/content/full/3/3/e1602244/DC1>

text S1. Sellers' two-stream approximation

text S2. 2D reflectance model

text S3. NIR_v and SIF simulations using SCOPE

table S1. Parameter values for two-stream approximation model.

table S2. Model parameters used in 2D reflectance model.
 table S3. Parameter ranges used in 2D reflectance model sensitivity test.
 table S4. SCOPE parameter values.
 table S5. Multiyear monthly average NIR_v, fPAR, and GPP, by land cover classification for 105 FLUXNET sites.
 fig. S1. NIR_v more strongly predicts canopy fPAR than does NDVI.
 fig. S2. NIR_v as a function of NDVI and NIR_r.
 fig. S3. Linear relationship between modeled NIR_v and SIF.
 fig. S4. Comparison of the monthly MODIS-derived (A) NIR_r and (B) NIR_v against GOME-2 measurements of SIF.
 References (37, 38)

REFERENCES AND NOTES

- C. B. Field, J. T. Randerson, C. M. Malmstrom, Global net primary production: Combining ecology and remote sensing. *Remote Sens. Environ.* **51**, 74–88 (1995).
- C. S. Potter, J. T. Randerson, C. B. Field, P. A. Matson, P. M. Vitousek, H. A. Mooney, S. A. Klooster, Terrestrial ecosystem production: A process model based on global satellite and surface data. *Global Biogeochem. Cycles* **7**, 811–841 (1993).
- G. D. Farquhar, S. von Caemmerer, J. A. Berry, A biochemical model of photosynthetic CO₂ assimilation in leaves of C₃ species. *Planta* **149**, 78–90 (1980).
- D. S. Schimel, J. I. House, K. A. Hibbard, P. Bousquet, P. Ciais, P. Peylin, B. H. Braswell, M. J. Apps, D. Baker, A. Bondeau, J. Canadell, G. Churkina, W. Cramer, A. S. Denning, C. B. Field, P. Friedlingstein, C. Goodale, M. Heimann, R. A. Houghton, J. M. Melillo, B. Moore, D. Murdiyarso, I. Noble, S. W. Pacala, I. C. Prentice, M. R. Raupach, P. J. Rayner, R. J. Scholes, W. L. Steffen, C. Wirth, Recent patterns and mechanisms of carbon exchange by terrestrial ecosystems. *Nature* **414**, 169–172 (2001).
- M. O. Smith, S. L. Ustin, J. B. Adams, A. R. Gillespie, Vegetation in deserts: I. A regional measure of abundance from multispectral images. *Remote Sens. Environ.* **31**, 1–26 (1990).
- D. S. Ellsworth, P. B. Reich, Canopy structure and vertical patterns of photosynthesis and related leaf traits in a deciduous forest. *Oecologia* **96**, 169–178 (1993).
- D. Y. Hollinger, Canopy organization and foliage photosynthetic capacity in a broad-leaved evergreen montane forest. *Funct. Ecol.* **3**, 53–62 (1989).
- P. J. Sellers, Canopy reflectance, photosynthesis and transpiration. *Int. J. Remote Sens.* **6**, 1335–1372 (1985).
- P. J. Sellers, Canopy reflectance, photosynthesis, and transpiration, II. The role of biophysics in the linearity of their interdependence. *Remote Sens. Environ.* **21**, 143–183 (1987).
- P. J. Sellers, J. A. Berry, G. J. Collatz, C. B. Field, F. G. Hall, Canopy reflectance, photosynthesis, and transpiration, III. A reanalysis using improved leaf models and a new canopy integration scheme. *Remote Sens. Environ.* **42**, 187–216 (1992).
- A. Porcar-Castell, E. Tyystjärvi, J. Atherton, C. van der Tol, J. Flexas, E. E. Pfündel, J. Moreno, C. Frankenberg, J. A. Berry, Linking chlorophyll a fluorescence to photosynthesis for remote sensing applications: Mechanisms and challenges. *J. Exp. Bot.* **65**, 4065–4095 (2014).
- L. Guanter, Y. Zhang, M. Jung, J. Joiner, M. Voigt, J. A. Berry, C. Frankenberg, A. R. Huete, P. Zarco-Tejada, J.-E. Lee, M. S. Moran, G. Ponce-Campos, C. Beer, G. Camps-Valls, N. Buchmann, D. Gianelle, K. Klumpp, A. Cescatti, J. M. Baker, T. J. Griffis, Global and time-resolved monitoring of crop photosynthesis with chlorophyll fluorescence. *Proc. Natl. Acad. Sci. U.S.A.* **111**, E1327–E1333 (2014).
- K. Guan, J. A. Berry, Y. Zhang, J. Joiner, L. Guanter, G. Badgley, D. B. Lobell, Improving the monitoring of crop productivity using spaceborne solar-induced fluorescence. *Glob. Chang. Biol.* **22**, 716–726 (2015).
- C. Frankenberg, J. B. Fisher, J. Worden, G. Badgley, S. S. Saatchi, J.-E. Lee, G. C. Toon, A. Butz, M. Jung, A. Kuze, T. Yokota, New global observations of the terrestrial carbon cycle from GOSAT: Patterns of plant fluorescence with gross primary productivity. *Geophys. Res. Lett.* **38**, L17706 (2011).
- J. Joiner, Y. Yoshida, A. P. Vasilkov, Y. Yoshida, L. A. Corp, E. M. Middleton, First observations of global and seasonal terrestrial chlorophyll fluorescence from space. *Biogeosciences* **8**, 637–651 (2011).
- C. Beer, M. Reichstein, E. Tomelleri, P. Ciais, M. Jung, N. Carvalhais, C. Rödenbeck, M. A. Arain, D. Baldocchi, G. B. Bonan, A. Bondeau, A. Cescatti, G. Lasslop, A. Lindroth, M. Lomas, S. Luuyssaert, H. Margolis, K. W. Oleson, O. Roupsard, E. Veenendaal, N. Viovy, C. Williams, F. I. Woodward, D. Papale, Terrestrial gross carbon dioxide uptake: Global distribution and covariation with climate. *Science* **329**, 834–838 (2010).
- C. B. Schaaf, F. Gao, A. H. Strahler, W. Lucht, X. Li, T. Tsang, N. C. Struwnell, X. Zang, Y. Jin, J.-P. Muller, P. Lewis, M. Barnsley, P. Hobson, M. Disney, G. Roberts, M. Dunderdale, C. Doll, R. P. d'Entremont, B. Hu, S. Liang, J. L. Privette, D. Roy, First operational BRDF, albedo nadir reflectance products from MODIS. *Remote Sens. Environ.* **83**, 135–148 (2002).
- R. Fensholt, I. Sandholt, M. S. Rasmussen, Evaluation of MODIS LAI, fAPAR and the relation between fAPAR and NDVI in a semi-arid environment using in situ measurements. *Remote Sens. Environ.* **91**, 490–507 (2004).
- D. Baldocchi, E. Falge, L. Gu, R. Olson, D. Hollinger, S. Running, P. Anthoni, C. Bernhofer, K. Davis, R. Evans, J. Fuentes, A. Goldstein, G. Katul, B. Law, X. Lee, Y. Malhi, T. Meyers, W. Munger, W. Oechel, K. T. Paw, K. Pilegaard, H. P. Schmid, R. Valentini, S. Verma, T. Vesala, K. Wilson, S. Wofsy, FLUXNET: A new tool to study the temporal and spatial variability of ecosystem-scale carbon dioxide, water vapor, and energy flux densities. *Bull. Am. Meteorol. Soc.* **82**, 2415–2434 (2001).
- S. W. Running, R. R. Nemani, F. A. Heinsch, M. Zhao, M. Reeves, H. Hashimoto, A continuous satellite-derived measure of global terrestrial primary production. *Bioscience* **54**, 547–560 (2004).
- C. B. Field, H. A. Mooney, The photosynthesis-nitrogen relationship in wild plants, in *On the Economy of Plant Form and Function*, T. J. Givnish, Ed. (Cambridge Univ. Press, 1986), pp. 25–55.
- A. J. Bloom, F. S. Chapin, H. A. Mooney, Resource limitation in plants—An economic analogy. *Annu. Rev. Ecol. Syst.* **16**, 363–392 (1985).
- S. V. Ollinger, A. D. Richardson, M. E. Martin, D. Y. Hollinger, S. E. Frolking, P. B. Reich, L. C. Plourde, G. G. Katul, J. W. Munger, R. Oren, M.-L. Smith, K. T. U. Paw, P. V. Bolstad, B. D. Cook, M. C. Day, T. A. Martin, R. K. Monson, H. P. Schmid, Canopy nitrogen, carbon assimilation, and albedo in temperate and boreal forests: Functional relations and potential climate feedbacks. *Proc. Natl. Acad. Sci. U.S.A.* **105**, 19336–19341 (2008).
- Y. Knyazikhin, M. A. Schull, P. Stenberg, M. Möttus, M. Rautiainen, Y. Yang, A. Marshak, P. Latorre Carmona, R. K. Kaufmann, P. Lewis, M. I. Disney, V. Vanderbilt, A. B. Davis, F. Baret, S. Jacquemoud, A. Lyapustin, R. B. Myneni, Hyperspectral remote sensing of foliar nitrogen content. *Proc. Natl. Acad. Sci. U.S.A.* **110**, E185–E192 (2013).
- D. G. G. de Pury, G. D. Farquhar, Simple scaling of photosynthesis from leaves to canopies without the errors of big-leaf models. *Plant Cell Environ.* **20**, 537–557 (1997).
- J. M. Chen, G. Mo, J. Pisek, J. Liu, F. Deng, M. Ishizawa, D. Chan, Effects of foliage clumping on the estimation of global terrestrial gross primary productivity. *Global Biogeochem. Cycles* **26**, GB1019 (2012).
- J. M. Norman, Interfacing leaf and canopy light interception models, in *Predicting Photosynthesis from Ecosystem Models*, J. D. Hesketh, J. W. Jones, Eds. (CRC Press, 1980), pp. 49–68.
- S. V. Ollinger, Sources of variability in canopy reflectance and the convergent properties of plants. *New Phytol.* **189**, 375–394 (2011).
- J. Joiner, L. Guanter, R. Lindstrot, M. Voigt, A. P. Vasilkov, E. M. Middleton, K. F. Huemmrich, Y. Yoshida, C. Frankenberg, Global monitoring of terrestrial chlorophyll fluorescence from moderate-spectral-resolution near-infrared satellite measurements: Methodology, simulations, and application to GOME-2. *Atmos. Meas. Tech.* **6**, 2803–2823 (2013).
- S. Hoyer, C. Fitzgerald, J. Hamman, Akleeman, T. Kluyver, M. Roos, J. J. Helmus, Markel, P. Cable, F. Maussion, xarray: v0.7.1 (2016).
- W. McKinney, Data structures for statistical computing in Python, in *Proceedings of the 9th Python in Science Conference*, S. van der Walt, J. Millman, Eds. (SciPy, 2010), pp. 51–56.
- S. van der Walt, S. C. Colbert, G. Varoquaux, The NumPy array: A structure for efficient numerical computation. *Comput. Sci. Eng.* **13**, 22–30 (2011).
- SymPy Development Team, *SymPy: Python Library for Symbolic Mathematics* (SymPy Development Team, 2016); www.sympy.org.
- J. D. Hunter, Matplotlib: A 2D graphics environment. *Comput. Sci. Eng.* **9**, 90–95 (2007).
- M. Waskom, O. Botvinnik, Drewokane, P. Hobson, Y. Halchenko, S. Lukuas, J. Warmenhoven, J. B. Cole, S. Hoyer, J. Vanderplas, S. Villalba, E. Quintero, M. Martin, A. Miles, K. Meyer, T. Augspurger, T. Yarkoni, P. Bachant, C. Evans, C. Fitzgerald, T. Nagy, E. Ziegler, T. Megjes, D. Wehner, S. St-Jean, L. P. Coelho, G. Hitz, A. Lee, Luc Rocher, seaborn: v0.7.0 (2016).
- F. Perez, B. E. Granger, IPython: A system for interactive scientific computing. *Comput. Sci. Eng.* **9**, 21–29 (2007).
- C. van der Tol, W. Verhoef, A. Rosema, A model for chlorophyll fluorescence and photosynthesis at leaf scale. *Agric. For. Meteorol.* **149**, 96–105 (2009).
- G. P. Asner, Biophysical and biochemical source of variation in canopy reflectance. *Remote Sens. Environ.* **64**, 234–253 (1998).

Acknowledgments: P. Sellers provided many constructive insights into the physical interpretation of NIR_v. We thank M. Whelan and L. Anderegg for the many discussions. N. Kasmalkar helped in framing several mathematical arguments. I. Woodrow provided critical feedback on our logic. The team at Google Earth Engine deserves special recognition for their efforts to support scientific research through access to large-scale computing. This work used eddy covariance data acquired and shared by the FLUXNET community, including the following networks: AmeriFlux, AfriFlux, AsiaFlux, CarboAfrica, CarboEuropeIP, CarboItaly, CarboMont, ChinaFlux, Fluxnet-Canada, GreenGrass, ICOS, KoFlux, LBA, NECC, OzFlux-TERN, TCOS-Siberia, and USCCC. The FLUXNET eddy covariance data processing and harmonization was carried out by the ICOS Ecosystem Thematic Center, AmeriFlux Management Project, and Fluxdata project of FLUXNET, with the support of CDIAC, and the OzFlux, ChinaFlux, and AsiaFlux offices. **Funding:** G.B. acknowledges support from

the NASA Earth and Space Science Fellowship. **Author contributions:** G.B. and J.A.B. conceived the experiment. G.B. collected the data and performed the analysis with help from J.A.B. All authors analyzed the results and contributed to writing of the manuscript. **Competing interests:** The authors declare that they have no competing financial interests. **Data and materials availability:** All data needed to evaluate the conclusions in the paper are present in the paper and/or the Supplementary Materials. Additional data related to this paper may be requested from the authors.

Submitted 14 September 2016
Accepted 9 February 2017
Published 22 March 2017
10.1126/sciadv.1602244

Citation: G. Badgley, C. B. Field, J. A. Berry, Canopy near-infrared reflectance and terrestrial photosynthesis. *Sci. Adv.* **3**, e1602244 (2017).